Int. J. Heat Mass Transfer. Vol. 14. pp. 1807–1824. Pergamon Press 1971. Printed in Great Britain.

CONVECTIVE HEAT TRANSFER IN A ROTATING RADIAL CIRCULAR PIPE (2ND REPORT)

Y. MORI and T. FUKADA
Faculty of Engineering, Tokyo Institute of Technology, Meguro-ku, Tokyo, Japan
and
W. NAKAYAMA
University of Alberta, Alberta, Canada

(*Received* 19 *October* 1970)

Abstract—In a straight circular pipe rotating around an axis perpendicular to its own axis, there occurs a secondary flow caused by Coriolis force, by which the flow resistance and the heat-transfer rate are increased. In this paper, first, the turbulent heat convection with fully developed velocity and temperature fields is theoretically studied by assuming a boundary layer along the wall. The increases in Nusselt number ratio Nu/Nu_0 and friction coefficient ratio λ/λ_0 for turbulent flow, where the denominators of the ratios are those without a secondary flow, are found to be less than in laminar region. Moreover no large circumferential variation of local Nusselt number is shown to exist.

Secondly, experimental results of heat-transfer coefficient, and those of local mass transfer coefficient by use of a naphthalene-sublimation technique in laminar and turbulent regions are reported. The theoretical result for friction coefficient agrees with the experimental data reported before. Our present experimental data on heat-transfer agree with the theoretical formulae for local and average Nusselt numbers reported in this paper and the 1st report.

NOMENCLATURE

A, w_1 at the pipe axis;
A', g_1 at the pipe axis;
a, radius of the pipe;
C, $\equiv -(\partial p'/\partial z)$;
C_p, specific heat of fluid at constant pressure;
C_{vw}, C_{vs}, density of stream at the wall surface and the flow core;
D, dimensionless velocity of the secondary flow in the flow core;
D_v, diffusion coefficient;
f_{zr}, $f_{z\psi}$, shear stress;
G, $T_w - T$;
g, dimensionless temperature, $\equiv G/\tau a$ (in the case of constant gradient of wall temperature), $G/(T_w - T_m)$ (in the case of constant wall temperature);
h_D, mass transfer coefficient;
k, thermal conductivity of fluid;
L, axial length of the measuring section;
$\dot{m}$, mass transfer rate per unit time per unit area;
N, $\hat{\omega}Re$;
Nu, Nusselt number, $\equiv 2aQ_{wm}/k(T_w - T_m)$;
Nu_a, analogous Nusselt number, $\equiv Sh(Pr/Sc)^l$;
Nu_0, Nusselt number without secondary flow;
n, speed of ratation;
n', constant defined by equation (62);
P, $\equiv (a^2/\nu^2)(p/\rho)$;
p', $p - (1/8)\hat{\omega}^2 z^2$;
Pr, Prandtl number;
p, pressure;
Q, heat flux;
g, dimensionless heat flux, $\equiv Q/k\tau$ (in the case of constant gradient of wall temperature), $aQ/k(T_w - T_m)$ (in the case of constant wall temperature);
g_w, $Q_w/k\tau$ (in the case of constant gradient of wall temperature), $aQ_w/k(T_w - T_m)$ (in the case of constant wall temperature);
Re, Reynolds number, $\equiv 2aW_m/\nu$;
R_v, gas constant;
r, radial co-ordinate in a cross section;

Sc, Schmidt number;
Sh, Sherwood number;
T, temperature;
U, r component of velocity, $u \equiv (a/\nu)\, U$;
V, ψ component of velocity, $v \equiv (a/\nu)\, V$;
v^*, w^*, ψ and z components of dimensionless friction velocity;
W, Z component of velocity, $w \equiv (a/\nu)\, W$;
W_m, mean velocity, $W_m \equiv (a/\nu)\, W_m$;
Z, axial co-ordinate, $z \equiv Z/a$.

Greek symbols

α, $\lambda_0 \equiv Re^{-1/m}$;
β, $Nu_0 \equiv \beta Pr^k Re^{(m-1)/m}$;
Γ, $\equiv Re/\hat{\omega}$ (inertia force)/(Coriolis force);
γ, specific weight;
δ, dimensionless thickness of the boundary layer;
η, $\equiv r/a$;
λ, resistance coefficient;
λ_0, λ without secondary flow;
λ^*, $\equiv (-\partial p'/\partial Z)\, 2a/(1/2)\, \rho W_m^2$;
ν, kinematic viscosity;
ξ, dimensionless distance from the pipe surface, $\equiv 1 - \eta$;
ρ, density;
τ, temperature gradient along the pipe axis;
τ, friction stress at the wall;
τ_{wz}, $\tau_{w\psi}$, axial and circumferential components of τ_w;
$\tau_{z\eta}$, $\tau_{z\psi}$, dimensionless shear stress in the axial direction;
ψ, circumferential co-ordinate in a cross section;
ω, angular velocity of the pipe, $\hat{\omega} \equiv 2a^2\omega/\nu$.

Subscripts

1, value in the flow core region;
4, value at $m = 4$;
5, value at $m = 5$;
m, mean value around the periphery (except g_m, T_m, V_m, W_m);
δ, value at $\xi = \delta$.

1. INTRODUCTION

IN A STRAIGHT circular pipe rotating around an axis perpendicular to its own axis, there occurs a secondary flow caused by the Coriolis force. An increase in the flow resistance and the heat-transfer rate, due to the secondary flow, can be expected. A study of the influence of the rotation of a pipe upon the heat-transfer rate has practical importance for the development of cooling techniques for rotating parts which become hot.

Our first report [1] presents a theoretical analysis in the fully developed laminar region. Approximate formulae for the Nusselt number in the case of an intense secondary flow caused by the Coriolis force are also reported.

Concerning the flow without heat-transfer in a rotating pipe, there are analytical reports by Ito and Nambu [2], and Barua [3] on the laminar region, but on the turbulent region no analysis has been made for the flow. The resistance coefficient for the flow without heat-transfer is experimentally obtained by Trefethen [4], and Ito and Nambu [5]. Experimental formulae for the resistance coefficient in the turbulent region are reported by the latter. However, no attention has been directed toward heat-transfer in a rotating pipe except in our first paper.

The object of the present study is: to make experiments on heat and mass transfer in a rotating pipe to experimentally examine the influence of the rotation upon heat-transfer in the laminar and turbulent regions; to compare these regions; to compare these experimental results of heat-transfer in the laminar region with a theoretical analysis discussed in the first report; and, to theoretically analyze velocity and temperature fields in the turbulent region and compare the results with experimental data.

2. THEORETICAL ANALYSIS OF THE FLOW IN A ROTATING PIPE IN THE TURBULENT REGION

2.1. *Co-ordinate and fundamental equations*

The system of the co-ordinates is taken as shown in Fig. 1. We assume $Z \gg r$. Since a secondary flow appears in the direction of the rotation of a pipe as seen in Fig. 1, an angle

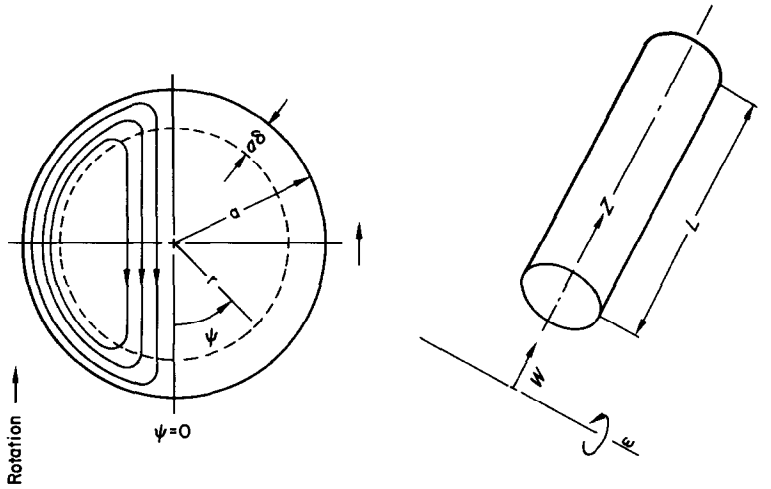

FIG. 1. System of co-ordinate.

measured from the secondary flow streamline passing through the center of the cross section is expressed by ψ.

r, ψ and Z components of velocity are denoted by U, V and W, respectively, the pressure by p, the density by ρ, and the kinematic viscosity by v. The dimensionless quantities are defined as follows;

$$\eta = r/a,\ z = Z/a,\ (u, v, w) = (a/v)(U, V, W)$$
$$\hat{\omega} = 2a^2\omega/v,\ P = (a^2/v^2)(p/\rho).$$

The pressure can be divided into two parts: one produced by the centrifugal force, and the other by the secondary flow. We write a dimensionless equation for P:

$$P = \tfrac{1}{8}\hat{\omega}^2 Z^2 + P'. \qquad (1)$$

The gradient of P' along the pipe axis (Z) is constant in the fully developed flow. Hence, we may put

$$-(\partial P'/\partial z) = C \quad \text{(constant)}.$$

The fluid discussed here is incompressible. The temperature difference between the fluid and the wall is small. Therefore, we disregard the physical property variation and the buoyancy effect, and analyze the fully developed velocity and temperature fields.

Shear stresses acting on the elemental volume of the fluid as shown in Fig. 2 are denoted by f_{zr} and $f_{z\psi}$. Their dimensionless quantities are expressed by $\tau_{z\eta} = (a^2/v^2)(f_{zr}/\rho)$ and $\tau_{z\psi} = (a^2/v^2)(f_{z\psi}/\rho)$. The force balance equation in the axial

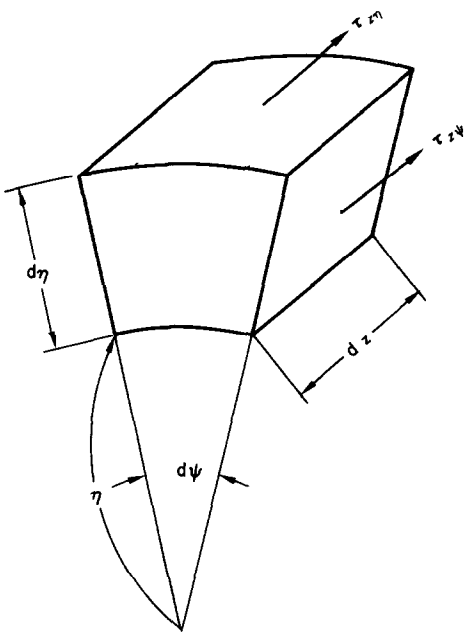

FIG. 2. Shear stresses acting on the elemental volume.

direction is represented in the following form:

$$\frac{\partial}{\eta\partial\eta}(\eta\tau_{z\eta}) + \frac{\partial\tau_{z\psi}}{\eta\partial\psi} = -C + \hat{\omega}(u\cos\psi - v\sin\psi) \quad (2)$$

where the seond term on the right-hand side of the equation signifies the Coriolis force acting in the axial direction due to the secondary flow.

In the turbulent flow, a dimensionless shear stress in the fluid is given by

$$\tau_{z\eta} = \frac{\partial w}{\partial\eta} - uw - \overline{u'w'}$$
$$\tau_{z\psi} = \frac{\partial w}{\eta\partial\eta} - vw - \overline{v'w'} \quad (3)$$

where time-averaged mean values are expressed by u, v, and w again, fluctuated velocities by u', v' and w', Reynolds stresses due to the turbulent fluctuation by $\overline{u'w'}$ and $\overline{v'w'}$.

Shear stresses uw and vw caused by the secondary flow are much stronger than the other stresses in most of the cross section, which is termed the flow core region. On the other hand, there is the very thin layer along the pipe wall, where we should pay attention to the stresses other than uw and vw. We call this region the boundary layer whose thickness is $a\delta$. When the pressure gradient in the axial direction is constant, δ varies not in the axial direction but only in the circumferential direction. However, the variation of δ is considered to be so small that δ is regarded as constant in the following analysis.

2.2. *Velocity distributions in the flow core region*

The velocity components u, v and w in the flow core region are denoted by u_1, v_1 and w_1. The dimensionless shear stresses in equation (3) are rewritten as:

$$\tau_{z\eta} = -u_1w_1$$
$$\tau_{z\psi} = -v_1w_1. \quad (4)$$

u_1, v_1 and w_1, which satisfy equations (3) and (4), the balance between the Coriolis force and a pressure gradient in the cross section, and moreover the equation of continuity, are given by

$$u_1 = D\cos\psi, v_1 = -D\sin\psi$$
$$w_1 = A + [(C/D) - \hat{\omega}]\eta\cos\psi \quad (5)$$

where A and D are constants.

2.3. *Friction stress at the wall and velocity distributions in the boundary layer*

If the friction stress at the wall, τ_w, and velocity distributions in the boundary layer are known, the relations between A and C in equation (5), and δ can be obtained. We adopt the dimensionless distance from the pipe wall $\xi = 1 - \eta$ in the following analysis.

The resistance coefficient formula for the flow without the secondary flow is

$$\lambda_0 = \alpha Re^{-1/m}. \quad (6)$$

The friction stress at the wall, τ_w, is derived from the above equation and the assumption of $1/(2m - 1)$ power velocity distribution [6]. α and m are constants. The value of m is usually 4 or 5. The subscript 0 means the resistance coefficient without the secondary flow. The Reynolds number is $Re = 2aW_m/\nu$.

The friction stress at the wall, τ_w concerns i and w. Since $v \ll w$, $\tau_{wz} \cong \tau_w$. Namely, the axial component of the friction stress at the wall is equal to the friction stress at the wall.

Dimensionless axial and circumferential components of τ_w are obtained from equation (6):

$$w^{*2} \equiv \left(\frac{a^2}{\nu^2}\right)\left(\frac{\tau_{wz}}{\rho}\right) = \frac{\alpha}{2^{3+(1/m)}}\left[\frac{(2m-1)^2}{m(4m-1)}\right]^{(2m-1)/m} A^{(2m-1)/m}\delta^{-1/m}\left[1 + \frac{2m-1}{m}\frac{1}{A}\left(\frac{C}{D} - \hat{\omega}\right)\cos\psi\right] \quad (7)$$

$$v^{*2} \equiv \left(\frac{a^2}{\nu^2}\right)\left(\frac{\tau_{w\psi}}{\rho}\right) = \frac{\alpha m}{2^{1+(1/m)}(2m-1)}\left[\frac{(2m-1)^2}{m(4m-1)}\right]^{(2m-1)/m} A^{(m-1)/m} \times \delta^{-(m+1)/m} \times D\left[1 + \frac{m-1}{m}\frac{1}{A}\left(\frac{C}{D} - \hat{\omega}\right)\cos\psi\right]\sin\psi \quad (8)$$

where w^* and v^* are components of dimensionless friction velocity.

w is defined from the condition of $w = w_{1\delta}$ (w_1 at $\xi = \delta$) at $\xi = \delta$ as:

$$w = w_{1\delta}(\xi/\delta)^{1/(2m-1)}. \tag{9}$$

v is determined so as to satisfy these conditions: $1/(2m-1)$ power law near the wall; $v = v_1$ at $\xi = \delta$; and, the continuity of the secondary flow rate.

$$v = -D\sin\psi\left[-\frac{m}{m-1}\left(\frac{2}{\delta}-1\right)\left(\frac{\xi}{\delta}\right)^{1/(2m-1)} + \frac{1}{m-1}\left(\frac{2m}{\delta}-1\right)\left(\frac{\xi}{\delta}\right)\right]. \tag{10}$$

We will find out the unknown quantities A and C. From equations (5) and (9), A is obtained as:

$$A = \frac{Re}{2}\frac{1}{1-(1/m)\delta+(1/4m-1)}\delta^2. \tag{11}$$

In consideration of the balance of forces of the fluid surrounded by the wall and two cross sections of a pipe, C is taken as:

$$C = 2w_m^{*2} \tag{12}$$

where the subscript m signifies a mean value around the periphery. From equation (12) and w_m^{*2} obtained from equations (7) and (11), we get

$$C = \frac{\alpha}{16}\left[\frac{(2m-1)^2}{m(4m-1)}\right]^{(2m-1)/m} Re^{(2m-1)/m}\,\delta^{-1/m}\left[1+\frac{2m-1}{m^2}\delta\right] \tag{13}$$

where we neglect smaller terms than δ^2 in (11):

2.4. *The boundary-layer momentum equations*

The relation between A, C and δ has been obtained. Since δ and D remain unknown quantities, we obtain them by using equations for the boundary layer momentum in the axial and circumferential directions.

The integral equation expressing the equilibrium of momentum in the axial direction is

$$w^{*2} = w_{1\delta}\frac{\partial}{\partial\psi}\int_0^\delta v\,\mathrm{d}\xi - \frac{\partial}{\partial\psi}\int_0^\delta vw\,\mathrm{d}\xi + \hat{\omega}\sin\psi\int_0^\delta v\,\mathrm{d}\xi + C\delta. \tag{14}$$

We substitute equations (5), (9) and (10) into the right-hand side of equation (14), then we get

$$w^{*2} = E + F\cos\psi \tag{15}$$

where

$$E = \left[\frac{6m-1}{(2m+1)(4m-1)}\cos^2\psi + \frac{4m(2m-1)}{(2m+1)(4m-1)}\sin^2\psi\right]D\left(\frac{C}{D}-\hat{\omega}\right) + \hat{\omega}D\sin^2\psi \tag{16}$$

$$F = \frac{6m-1}{(2m+1)(4m-1)}AD. \tag{17}$$

It is clear from equation (16) that the mean value of w^{*2}, i.e. $w_m{}^{*2}$, satisfies equation (12). The variation of E with ψ is smaller than that of $F\cos\psi$ in equation (16). Therefore, it is possible to replace E with its mean value, $C/2$. We put equation (15) equal to equation (7) and substitute equation (11) and (13) into them. Then we get

$$D\delta^{1/m} = \frac{\alpha}{8}\left[\frac{(4m^2-1)(4m-1)}{2m(6m-1)}\right]^{\frac{1}{2}} \times\left[\frac{(2m-1)^2}{m(4m-1)}\right]^{(2m-1)/m} Re^{(m-1)/m}\chi' \tag{18}$$

where

$$\chi' = \left[1+\frac{(4m^2-1)(4m-1)}{2m(6m-1)}\left(\frac{\hat{\omega}}{Re}\right)^2\right]^{\frac{1}{2}} - \left[\frac{(4m^2-1)(4m-1)}{2m(6m-1)}\right]^{\frac{1}{2}}\left(\frac{\hat{\omega}}{Re}\right). \tag{19}$$

The parameter χ' represents the effect of the Coriolis force acting on the secondary flow.

The momentum equation in the circumferential direction is expressed by

$$v^{*2} = -\int_0^\delta \frac{dP_\delta}{d\psi}\,d\xi - \hat{\omega}\sin\psi\int_0^\delta w\,d\xi + v_1\frac{\partial}{\partial\psi}\int_0^\delta v\,d\xi - \frac{\partial}{\partial\psi}\int_0^\delta v^2\,d\xi \qquad (20)$$

where P_δ is the value of P_1 at $\xi = \delta$.

We may consider that δ itself is the mean value of the boundary layer thickness around $\psi = -\pi \sim \pi$. Then we get

$$D\delta^{-(2m+1)/m} = \frac{2m-1}{m^2\alpha}\left[\frac{(2m-1)^2}{m(4m-1)}\right]^{-(2m+1)/m} \times Re^{1/m}\hat{\omega}. \qquad (21)$$

From equations (18) and (21), D and δ are obtained as:

$$D = \hat{D}Re^{m/(m+1)}\Gamma^{-\frac{1}{2}(m+1)}\chi'^{(2m+1)/2(m+1)} \qquad (22)$$

where

$$\log\hat{D} = \frac{1}{m+1}\left[\frac{1}{4}\{(2m+1)\log(2m+1) - (10m+1)\log m + (18m-5)\log(2m-1) - (6m-5)\log(4m-1) - (2m+1)\log(6m-1) - 7(2m+1)\log 2\} + m\log\alpha\right] \qquad (23)$$

$$\delta = \hat{\delta}\left(\frac{\Gamma^{m/2}\chi'^{m/2}}{Re}\right)^{1/(m+1)} \qquad (24)$$

where

$$\log\hat{\delta} = \frac{1}{m+1}\left[\frac{1}{4}\{m\log(2m+1) - (5m-4)\times\log m + (15m-8)\log(2m-1) - (7m-4)\log(4m-1) - m\log(6m-1) - 7m\log 2\} + m\log\alpha\right]. \qquad (25)$$

The parameter Γ in equations (22) and (24) is expressed by

$$\Gamma = Re/\hat{\omega} = W_m/aw. \qquad (26)$$

The physical meaning of which is the ratio of the inertia force to the Coriolis force.

2.5. *Resistance coefficient*

The resistance coefficient λ is defined as follows:

$$\lambda \equiv \left(-\frac{\partial p}{\partial Z}\right)2a/(1/2)\rho W_m^2 \qquad (27)$$

which can also be rewritten in the following form by use of equation (1):

$$\lambda \equiv -4\frac{\hat{\omega}^2}{Re^2}Z + \lambda^* \qquad (28)$$

where

$$\lambda^* \equiv \left(-\frac{\partial p'}{\partial Z}\right)2a/(1/2)\rho W_m^2. \qquad (29)$$

The first and the second terms on the right-hand side of equation (28) correspond to the pressure rise caused by the centrifugal force and the secondary flow, respectively. Then we rewrite λ^* as:

$$\lambda^* = 16C/Re^2. \qquad (30)$$

We put equation (13) into equation (30) by use of equation (24).

$$\lambda^*[\Gamma\chi']^{\frac{1}{2}} = \frac{\hat{\lambda}^*}{(Re/\Gamma^{m/2}\chi'^{m/2})^{1/(m+1)}} \times\left[1 + \frac{\Delta\lambda^*}{(Re/\Gamma^{m/2}\chi'^{m/2})^{1/(m+1)}}\right] \qquad (31)$$

where

$$\log\hat{\lambda}^* = \frac{1}{m+1}\left[\frac{1}{4}\{-\log(2m+1) - (8m-1)\log m + (16m-7)\log(2m-1) - (8m-3)\log(4m-1) + \log(6m-1) + 7\log 2\} + m\log\alpha\right] \qquad (32)$$

$$\log\Delta\lambda^* = \frac{1}{m+1}\left[\frac{1}{4}\{m\log(2m+1) - (13m+4)\log m + (19m-4)\log(2m-1) - (7m-4)\log(4m-1) - m\log(6m-1) - 7m\log 2\} + m\log\alpha\right]. \qquad (33)$$

λ_0 and λ^* at $m = 4$ are expressed by λ_{04} and λ_4^*. α is determined to be 0·305 (the value corrected from 0·316) in comparison with usual experimental results. So we get as:

$$\lambda_4^* [\Gamma\chi_4']^{\frac{1}{4}} = \frac{0{\cdot}304}{(Re/\Gamma^2\chi_4'^2)^{\frac{1}{4}}}\left[1 + \frac{0{\cdot}107}{(Re/\Gamma^2\chi_4'^2)^{\frac{1}{4}}}\right] \quad (34)$$

where χ_4' is

$$\chi_4' = [1 + 5{\cdot}14/\Gamma^2]^{\frac{1}{4}} - 2{\cdot}27/\Gamma. \quad (35)$$

The result of equation (34) is shown and compared with experimental results obtained by Trefethen [4] in Fig. 3. Good agreement is found between the theoretical curve and experimental values by Trefethen for the large length-to-diameter ratios, 60 and 87. However, data for the small ratio lie between the theoretical curve and that for a case without the secondary flow. This implies that the secondary flow is not fully developed.

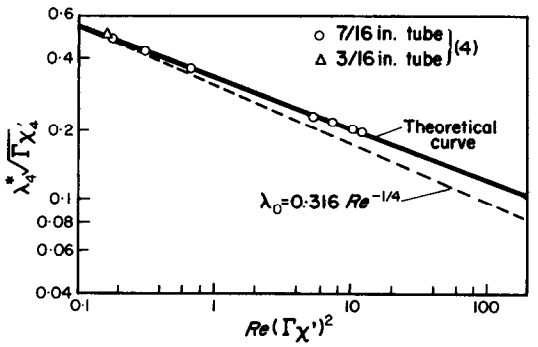

FIG. 3. $\lambda_4^*/\Gamma\chi_4'$ vs. $Re/\Gamma^2\chi'^2$.

When Re and $\hat{\omega}$ are considerably large, $\lambda_{05} = 0{\cdot}184\, Re^{-\frac{1}{4}}$ (at $m = 5$). From this formula, we may put $m = 5$ and $\alpha = 0{\cdot}184$ and get

$$\lambda_5^* [\Gamma\chi_5']^{\frac{1}{4}} = \frac{0{\cdot}194}{(Re/\Gamma^{2{\cdot}5}\chi_5'^{2{\cdot}5})^{\frac{1}{4}}} \times \left[1 + \frac{0{\cdot}066}{(Re/\Gamma^{2{\cdot}5}\chi_5'^{2{\cdot}5})^{\frac{1}{4}}}\right] \quad (36)$$

where χ_5' is

$$\chi_5' = [1 + 6{\cdot}49/\Gamma^2]^{\frac{1}{4}} - 2{\cdot}55/\Gamma. \quad (37)$$

The numerical check of λ_4^* and λ_5^* suggests that λ_4^* is valid for practical use except for the case of extremely large Re and $\hat{\omega}$. The ratio of λ_4^* at $m = 4$ to the resistance coefficient without the secondary flow, λ_4^*/λ_{04}, is shown in Fig. 4.

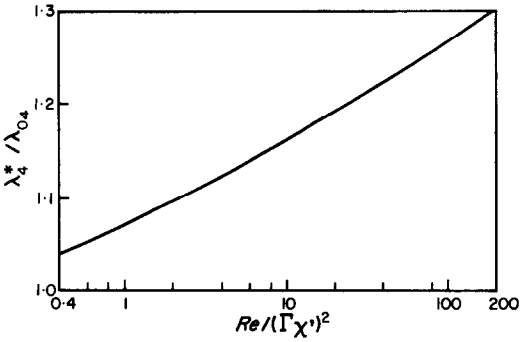

FIG. 4. λ_4/λ_0 vs. $Re/\Gamma^2\chi'^2$.

3. HEAT TRANSFER IN THE TURBULENT REGION IN A ROTATING PIPE

3.1. *Fundamental equations*

In the case of a constant gradient of wall temperature along the pipe axis, the temperature T in the fully developed temperature field is written as follows:

$$T = \tau Z - G(r, \psi) \quad (38)$$

where τ denotes the uniform wall temperature gradient along the pipe axis per unit length and G is a function of r and ψ.

It may be assumed that the wall temperature remains the same in the direction of ψ. Therefore, we put T_w as $T_w = \tau Z$.

If the dimensionless temperature is expressed by $g = G/\tau a$, the energy equation is written as:

$$\frac{\partial}{\eta\partial\eta}(\eta q_\eta) + \frac{\partial q_\psi}{\eta\partial_\psi} = Prw \quad (39)$$

where q_η and q_ψ are the dimensionless quantities defined by $q_\eta = Q_\eta/k\tau$ and $q_\psi = Q_\psi/k\tau$, and Q_η and Q_ψ are heat fluxes in radial and circumferential directions. q_η and q_ψ are also expressed by

$$q_\eta = -\frac{\partial g}{\partial\eta} + Pr(ug + \overline{u'g'})$$
$$q_\psi = -\frac{\partial g}{\eta\partial\psi} + Pr(vg + \overline{v'g'}) \quad (40)$$

where g and g' respectively represent the time-averaged mean value and the fluctuated value of temperature.

We will define the dimensionless temperature for the case of the constant wall temperature [7].

$$g = (T_w - T)/(T_w - T_m)$$

where T_m is the mixed mean temperature defined below.

$$T_m = \frac{1}{\pi a^2 W_m} \int_{\pi}^{\pi} \int_{0}^{a} TWr\mathrm{d}r\mathrm{d}\psi. \tag{41}$$

T can be expressed by the form of $T_w - T \propto \exp(-e'Z)$ using an eigen value e' in the region far from the entrance of a pipe [7]. Therefore, when the dimensionless heat fluxes and the dimensionless eigen value are defined as $q_\eta = aQ_\eta/k(T_w - T_m)$, $q_\psi = aQ_\psi/k(T_w - T_m)$ and $e = ae'$ in case of the constant wall temperature, q_η and q_ψ are written in the same form as equation (40) and the energy equation is obtained by replacing Prw by $ePrwg$ on the right-hand side of equation (39).

3.2. *Temperature distribution in the flow core region*

Heat transfer caused mainly by a secondary flow appears in the flow core region. From equation (40) we get

$$q_\eta = Pru_1 g_1, \; q_\psi = Prv_1 g_1. \tag{42}$$

In the case of a uniform τ, the substitution of equation (42) into equation (39) leads to the particular solution

$$g_1 = A' + \frac{1}{2D}\left(\frac{C}{D} - \hat{\omega}\right)\eta^2 + \frac{A}{D}\eta\cos\psi \tag{43}$$

where A' is a constant.

In the case of a uniform T_w, the solution is obtained from the energy equation and equation (42) as follows:

$$g_1 = \bar{N}\exp\left[\frac{e}{D}\left\{A + \frac{1}{2}\left(\frac{C}{D} - \hat{\omega}\right)\eta\cos\psi\right\}\eta\cos\psi\right] \tag{44}$$

where $\bar{N}$ is a constant to be determined by the definition of so as to satisfy a normalized condition below.

$$\frac{2}{\pi Re}\int_{-\pi}^{\pi}\int_{0}^{1} wg\eta\mathrm{d}\eta\mathrm{d}\psi = 1. \tag{45}$$

Equation (44) can be expanded because the variation of temperature in the cross section of the flow core is assumed to be small.

$$g_1 = \bar{N}\left[1 + \frac{eA}{D}\eta\cos\psi + \frac{e}{2D}\left\{\left(\frac{C}{D} - \hat{\omega}\right) + \frac{eA^2}{D}\right\}\eta^2\cos^2\psi + \frac{e^2A}{2D^2}\left\{\left(\frac{C}{D} - \hat{\omega}\right) + \frac{eA^2}{3}\right\}\eta^3\cos^3\psi + \ldots\right] \tag{46}$$

We assume $\delta \ll 1$ and substitute w_1 and g_1 into equation (45). We have

$$\bar{N} = \frac{1}{1 + \frac{3}{8}\frac{e}{D}\left(\frac{C}{D} - \hat{\omega}\right) + \frac{1}{8}\frac{e^2A^2}{D^2}}. \tag{47}$$

3.3. *Determination of the dimensionless heat flux at the wall, q_w, and the constants A' and e.*

The definition of the Nusselt number is

$$Nu = \frac{2aQ_{wm}}{k(T_w - T_m)} \tag{48}$$

where Q_{wm} is the mean value of Q_w around the periphery of a cross section ($\psi = -\pi \sim \pi$).

When the dimensionless heat fluxes at the wall for the uniform τ and uniform T_w cases are written as $q_w = Q_w/k\tau$ and $q_w = aQ_w/k(T_w - T_m)$ respectively, the Nusselt number for a case without a secondary flow is given as follows:

$$Nu_0 = \beta Pr^\kappa Re^{(m-1)/m}. \tag{49}$$

The dimensionless heat flux is also expressed for both wall temperature conditions as:

$$q_w = q_w Pr^\kappa A^{(m-1)/m}\delta^{-1/m} g_{1\delta}\left[1 + \frac{m-1}{m}\frac{1}{A}\times\left(\frac{C}{D} - \hat{\omega}\right)\cos\psi\right] \tag{50}$$

where β and k are constants, $g_{1\delta}$ is the value of g_1 at $\xi = \delta$, and

$$\hat{q}_w = 2^{-(m+1)/m} \left\{\frac{(2m-1)^2}{m(4m-1)}\right\}^{(m-1)/m} \frac{4m-1}{2m-1}\beta \quad (51)$$

The values of m, β and k in the case where $Pr \geqslant 1$ are scarcely influenced by wall temperature conditions. Therefore, we may use the same symbols for both wall temperature conditions of the uniform τ and the uniform T_w and adopt equations (50) and (51) in the following analysis.

The equation describing the heat balance of the fluid element in the unit length of the pipe is given by

$$\int_{-\pi}^{\pi} Q_w a \mathrm{d}\psi = \rho C_p \frac{\partial}{\partial Z} \int_{-\pi}^{\pi}\int_{0}^{a} TW r \mathrm{d}r\mathrm{d}\psi. \quad (52)$$

Equation (52) can be rewritten in the following forms for each wall temperature condition by using dimensionless quantities.

The equation for the uniform τ case is

$$q_{wm} = (1/4)\, Re\,.\, Pr \quad (53)$$

and for the uniform T_w case is

$$q_{wm} = (1/4)\, eRePr. \quad (54)$$

q_{wm} denotes the mean value of q_w around the periphery of a cross section in both equations.

The value of $g_{1\delta}$ for the uniform τ case can be obtained by putting $\eta = 1 - \delta$ into equation (43).

$$g_{1\delta} = A' + \frac{1}{2D}\left(\frac{C}{D} - \hat{\omega}\right)(1-\delta)^2 + \frac{A}{D}(1-\delta)$$
$$\cos\psi \cong A' + \frac{1}{2D}\left(\frac{C}{D} - \hat{\omega}\right) + \frac{A}{D}\cos\psi. \quad (55)$$

We can get the value of $g_{1\delta}$ for the uniform T_w case from equation (46) in the same way as before.

$$g_{1\delta} = \bar{N}\left[1 + \frac{e}{2D}\left(\frac{C}{D} - \hat{\omega} + \frac{eA^2}{D}\right)(1-\delta)^2 \times \cos^2\psi + \frac{eA}{D}\left\{(1-\delta) + \frac{e}{2D}\left(\frac{C}{D} - \hat{\omega} + \frac{eA^2}{3D}\right)(1-\delta)^3 \cos^2\psi\right\} \times \cos\psi\right]$$
$$\cong \bar{N}\left[1 + \frac{e}{4D}\left(\frac{C}{D} - \hat{\omega}\right) + \frac{e^2A^2}{4D^2}\right] + \frac{eA}{D}\bar{N} \times \left[1 + \frac{e}{4D}\left(\frac{C}{D} - \hat{\omega}\right) + \frac{e^2A^2}{6D^2}\right]\cos\psi$$
$$\cong 1 + (eA/D)\cos\psi. \quad (56)$$

For the uniform τ case, equation (55) is substituted into equation (50), q_{wm} obtained from equation (50) into equation (53) and neglect smaller terms than δ^2 to get A'.

$$A' = (Pr^{1-\kappa} - \Delta A')\frac{A'}{1 + \dfrac{m-1}{m^2}\delta} Re^{1/(m+1)} (\Gamma\chi')^{\frac{1}{2}(m+1)} \quad (57)$$

where $\hat{A}'$ and $\Delta A'$ are given below.

$$\log \hat{A}' = \frac{1}{m+1}\left[\frac{1}{4}\{(4m+5)\log(2m+1) + (4m-5)\log m - (8m-15)\log(2m-1) - 11\log(4m-1) - \log(6m-1) - 7\log 2\} + \log\alpha\right] - \log\beta \quad (58)$$

$$\Delta A' = \frac{4m(4m-1)(6m-1)}{(2m+1)^2(2m-1)^2}\frac{\beta}{\alpha}. \quad (59)$$

For the uniform T_w case, the same way is applied to get

$$\Delta e = \frac{4m(4m-1)(6m-1)(m-1)}{(2m+1)^2(2m-1)^3}\frac{\beta}{\alpha}. \quad (60)$$

The value obtained by substituting Δe into $\Delta A'$ in equation (57) is equal to $1/e$. Since these correction terms $\Delta A'$ and Δe are small, A' and $1/e$ are nearly equal.

3.4. *Energy integral equations in the boundary layer*

The energy integral equation for the uniform τ case is given as:

$$q_w/Pr = g_{1\delta}\frac{\partial}{\partial\psi}\int_0^{\delta} v\mathrm{d}\xi - \frac{\partial}{\partial\psi}\int_0^{\delta} gv\mathrm{d}\xi + \int_0^{\delta} w\mathrm{d}\xi. \quad (61)$$

For the uniform T_w case, the energy integral equation is obtained by replacing the third term on the right-hand side of equation (61) by $e\int_0^\delta wg\mathrm{d}\xi$.

However, convective terms due to w, i.e. $\int_0^\delta w\mathrm{d}\xi$ and $e\int_0^\delta wg\mathrm{d}\xi$, are negligibly small.

The temperature distribution in the boundary layer is assumed to be

$$g = g_{1\delta}(\xi/\delta)^{1/n'} \tag{62}$$

where n' is an unknown quantity to be obtained.

From equation (50), q_w can be rewritten in the following forms. For the uniform τ case, we have

$$q_w = q_{wm} + q'_w \cos\psi. \tag{63}$$

For the uniform T_w case, we have

$$q_w = q_{wm} + q'_w e\cos\psi \tag{64}$$

where

$$q'_w = \hat{q}_w Pr^{\kappa} A^{(m-1)/m-1/m}(A/D).$$

We substitute equations (10) and (62) into equation (61) and for the uniform τ case, we have

$$q_w = q_{wm} + q''_w A'\cos\psi. \tag{65}$$

For the uniform T_w case, we have

$$q_w = q_{wm} + q''_w\cos\psi \tag{66}$$

where

$$q''_w = Pr\left[1 - \frac{2m}{m-1}\left(\frac{1}{\frac{1}{n'}+\frac{1}{2m-1}+1} - \frac{1}{\frac{1}{n'}+2}\right)\right]. \tag{67}$$

Therefore, n' can be obtained by putting equation (63) equal to equation (65) or equation (64) to equation (66). The equation for n' is the same for both wall temperature conditions because of the relationship $A' \cong 1/e$. The following equation for n' for the uniform τ case is also applicable to the uniform T_w case.

$$n' \cong 2m - 1. \tag{68}$$

3.5. *Nusselt numbers*

For the uniform τ case, equation (48) can be expressed in the dimensionless form as:

$$Nu = \frac{2q_{wm}}{g_m} = \frac{RePr}{2g_m} \tag{69}$$

where g_m is defined as:

$$g_m = \frac{2}{\pi Re}\left\{\int_{-\pi}^{\pi}\int_0^{1-\delta} g_1 w_1 \eta\mathrm{d}\eta\mathrm{d}\psi + \int_{-\pi}^{\pi}\int_0^{\delta} gw(1-\xi)\mathrm{d}\xi\mathrm{d}\psi\right\}. \tag{70}$$

For the uniform T_w case, we have

$$Nu = \frac{RePre}{2}. \tag{71}$$

It is clear from equations (69) and (71) that $1/e$ corresponds to g_m. However, the substitution of equations (50), (9), (43), (62) and (68) into equation (70) shows that A' is a governing factor in g_m. Therefore, the wall temperature condition has no influence on the Nusselt number since $A' \cong 1/e$. We will discuss the Nusselt numbers for the uniform τ case in the following analysis.

The Nussett number is derived from equation (69) and (70).

$$Nu = \frac{1}{2\hat{A}}\frac{Pr}{Pr^{1-k}\Delta g_m}\frac{Re^{m/(m+1)}}{(\hat{\Gamma}\chi')^{1/2(m+1)}}\left[1 + \frac{\Delta Nu}{\left(\frac{Re}{\Gamma^{m/2}\chi'^{m/2}}\right)^{1/(m+1)}}\right] \tag{72}$$

where correction terms Δg_m and ΔNu are given by

$$\Delta g_m = \frac{4m(m-1)(4m-1)(6m-1)}{(2m+1)^2(2m-1)^3}\frac{\beta}{\alpha} \tag{73}$$

$$\Delta Nu = \frac{4m^2-2m-1}{m^2(2m+1)}\delta. \tag{74}$$

The ratio of the Nusselt number to that without a secondary flow is

$$\frac{Nu}{Nu_0} = \frac{Pr^{1-\kappa}}{2\hat{A}'\beta(Pr^{1-\kappa}\Delta g_m)}\left(\frac{Re}{\Gamma^{m/2}\chi'^{m/2}}\right)^{1/m(m+1)}\left[1+\frac{\Delta Nu}{\left(\frac{Re}{\Gamma^{m/2}\chi'^{m/2}}\right)^{1/(m+1)}}\right]. \quad (75)$$

For a case of $Pr \cong 1$, from $m = 4$, $\alpha = 0{\cdot}305$, $\beta = 0{\cdot}038$ and $k = 1/3$ we obtain

$$Nu_4 = \frac{0{\cdot}039Pr}{Pr^{\frac{2}{3}} - 0{\cdot}074}\frac{Re^{\frac{4}{5}}}{(\hat{\Gamma}\chi_4')^{\frac{1}{10}}}\left[1+\frac{0{\cdot}093}{\left(\frac{Re}{\Gamma^2\chi_4'^2}\right)^{\frac{1}{5}}}\right]. \quad (76)$$

For a case of $Pr > 1$, from the relation between $m = 5$, $\alpha = 0{\cdot}184$, $\beta = 0{\cdot}023$ and $k = 0{\cdot}4$ and $Pr^{1-k}/(Pr^{1-k} - \Delta g_m) \cong 1$ we get

$$Nu_5\, Pr^{0{\cdot}4} = 0{\cdot}025\frac{Re^{\frac{4}{5}}}{(\Gamma\chi_5')^{\frac{1}{12}}}\left[1+\frac{0{\cdot}059}{\left(\frac{Re}{\Gamma^{2{\cdot}5}\chi_5'^{2{\cdot}5}}\right)^{\frac{1}{5}}}\right]. \quad (77)$$

The ratio of Nu/Nu_0 for $Pr \cong 1$ is illustrated in Fig. 5 and for $Pr > 1$ in Fig. 6.

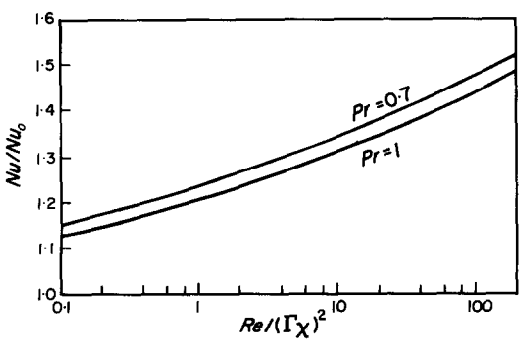

FIG. 5. Nu/Nu_0 vs. $Re/\Gamma^2\chi'^2$ at $Pr = 0{\cdot}7$ and 1.

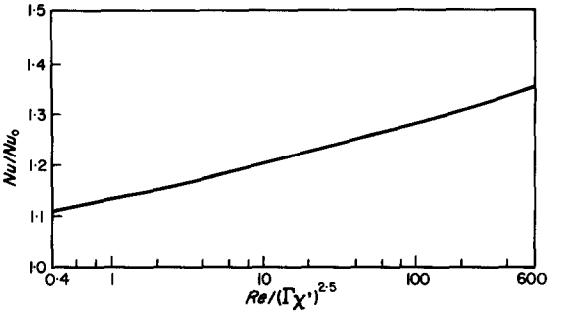

FIG. 6. Nu/Nu_0 vs. $Re/\Gamma^{2{\cdot}5}\chi'^{2{\cdot}5}$.

4. EXPERIMENTS

4.1. *Experimental apparatus*

The experimental apparatus is drawn in Fig. 7. It is divided into a rotating body and two measuring parts (1), (2) as shown in Fig. 8. We can vary the speed of rotation of the body by a motor (3) from 0 to 1000 rpm. The slip-ring mechanisms (7), (8) are used for the heat-input and the measurement of temperature. The input can be adjusted by the slidacs. A compensating circuit is set to correct errors of the temperature measurement due to a temperature rise at a slip-ring. The air sent from a compressor enters the straight pipes (1), (2) after it travels trough a flow meter (5), an air-input apparatus having a seal mechanism (6), and the rotating body. A flow rectifier is set at the entrance to the part which measures the heat-transfer rate to minimize the influence of the curvature of this apparatus upon the inflow of the air.

The measuring parts consist of those for heat and mass transfer rates as shown in Fig. 8.

The measuring part for the mass transfer rate is divided into two semicylinders suitable for the measurement of the rate of sublimation by using the naphthalene-sublimation technique. Naphthalene with a 6 mm i.d. and a 3·5 mm thickness is cast onto the inner wall of the brass semicylinder, which is covered with three heaters to keep the wall temperature constant in the direction of the flow. Moreover, an insulator covers these heaters.

We put thermo-couples within the naphthalene layer to measure the temperature at the surface

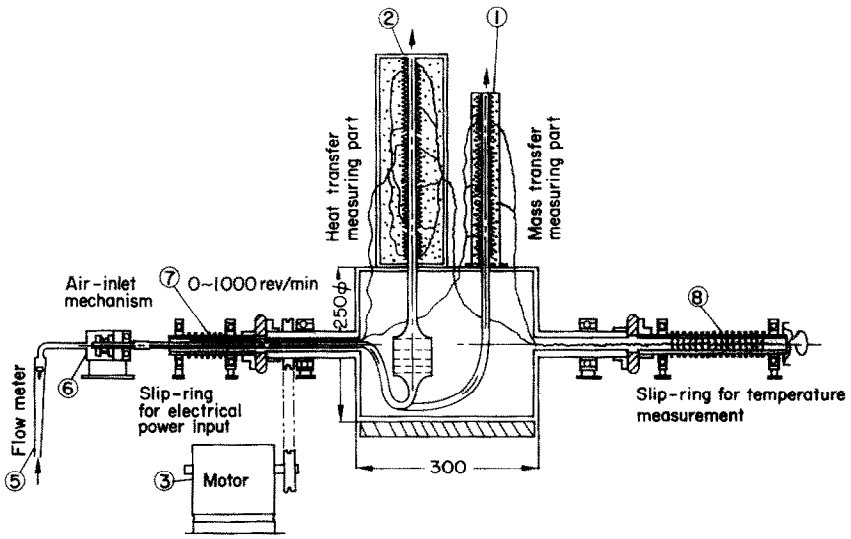

FIG. 7. Experimental apparatus.

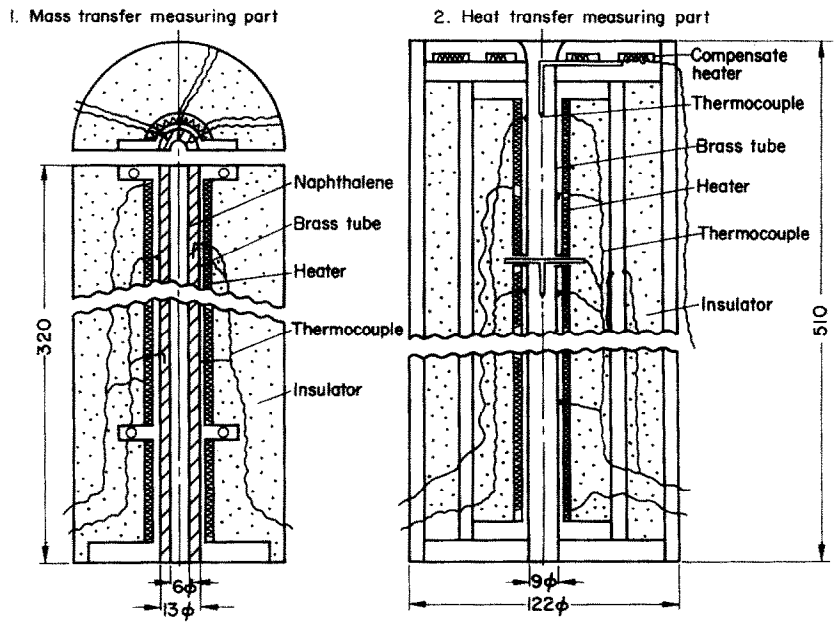

FIG. 8. Detailed measuring parts.

by extrapolating from a temperature drop within this layer. The wall temperature is measured at four positions along the pipe axis and at six positions in the circumferential direction at one of the four axial positions.

The thickness of sublimation of the naphthalene is measured by using a micrometer with a special attachment suitable for the measurement.

The measuring part for the heat transfer rate is a straight brass pipe with a 9 mm i.d. The outer

surface of the pipe is covered with seven separate heaters in the axial direction. An insulator is used around the heaters. A sub-heater is attached at the exit part of the pipe to prevent heat loss. Measurement of the wall temperature is made at nine positions in the axial direction. The temperature distribution is obtained in the circumferential direction at three positions among the nine mentioned above. The temperature at the center is measured at two positions in the fully developed field on the pipe axis.

4.2. *Measuring method and arrangement*

The mass transfer coefficient for the experiments on mass transfer is defined as:

$$\dot{m} = h_D(C_{vw} - C_{vs}) \tag{78}$$

where $\dot{m}$ is the rate of sublimation per unit time and unit area, and C_{vw} and C_{vs} denote the concentrations of naphthalene vapor at the naphthalene surface and in the flow core region. C_{vw} and C_{vs} can be expressed as follows by using the well-known relationship.

$$C_{vw} = \frac{P_{vw}}{R_v T_w}, C_{vs} = \frac{M}{V_m} \tag{79}$$

where P_{vw} describes the vapor pressure at the naphthalene surface, R_v the gas constant, M the total rate of sublimation up to the measuring position and V_m the mean flow rate of the fluid.

The rate of sublimation $\dot{m}$ is expressed as follows in the measurement of the naphthalene thickness.

$$\dot{m} = \gamma S \tag{80}$$

where γ denotes the specific weight and S the thickness of naphthalene sublimation.

The mass transfer coefficient n_D is derived from equations (78)–(80)

$$h_D = \frac{\gamma S}{\dfrac{P_{vw}}{R_v T_w} - \dfrac{M}{V_m}}. \tag{81}$$

The analogous Nusselt number is defined by using the analogy between mass and heat transfer.

$$Nu_a = Sh(Pr/Sc)^l \tag{82}$$

where Sh expresses the Sherwood number $\equiv 2ah_D/D_v$, Pr the Prandtl number, Sc the Schmidt number $= 2{\cdot}6$ l is a transformation exponent, the value of which is usually determined as $l = 1/3$ for the forced convection. We also adopt this value for both laminar and turbulent regions in this paper.

The experiments are made under these conditions; the speed of rotation $n = 0 \sim 1000$ rpm.; $Re = 1000 \sim 10800$; $T_w = 25 \sim 45°C$; and the measuring time lasts 3 h. We neglect the rate of sublimation during the measurement of the naphthalene thickness sublimated because it is considered to be a little less than 5 per cent of that during the pipe rotation.

The Nusselt number for the experiments on heat transfer is defined in the following equation.

$$Nu = 2aQ_{wm}/k(T_w - T_m) \tag{83}$$

for the fully developed velocity and temperature distributions is written as:

$$Q_{wm} = (1/2)\tau a W_m \gamma C_p \tag{84}$$

where τ is the temperature gradient in the axial direction, W_m the mean velocity, γ the specific weight and C_p the specific heat.

According to the results of the measurement of temperature, the temperature gradient of the pipe wall toward the axial direction agrees with that at the center of the pipe. Since the difference found between temperatures at the center obtained theoretically and experimentally is within 10 per cent, T_m is obtained from the velocity and temperature distributions assumed and the temperature at the center experimentally measured.

5. EXPERIMENTAL RESULTS

5.1. *Experiments in the laminar region*

(i) *Experiments for calibration (Experiments when a pipe is not rotating).* We made experiments on forced convective heat-transfer, when a pipe is not rotating, to examine the accuracy of our measurements. The local Nusselt number taken

in the radial direction in the cross section at $Z/L = 0{\cdot}63$, when the pipe is not rotating, i.e. without a secondary flow, is illustrated in Fig. 9. The solid line in the figure represents the solution of the Nusselt number for the constant wall temperature with the parabolic velocity distribution. The experimental results agree well with this solution and have little

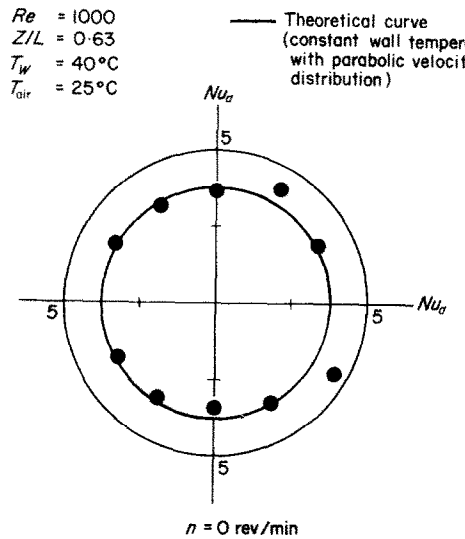

FIG. 9. Local mass transfer result in laminar region (no rotation).

variation in the circumferential direction. The analogous Nusselt number in the direction of the flow agrees well with the theoretical solution when the pipe is not rotating. It is clear from the experimental results mentioned above that the experimental apparatus and the measuring methods are suitable for our study.

(ii) *Experiments when a pipe is rotating.* One of the experimental results when the pipe is rotating is given in Fig. 10. It shows the local Nusselt number by equation (82) in the cross section at $Z/L = 0{\cdot}63$, where the velocity field is considered to be fully developed. The solid line in the figure represents the theoretical solution obtained in the first report and the dotted line the solution when the pipe is not rotating. Good agreement is seen between the experimental results and the theoretical solution,

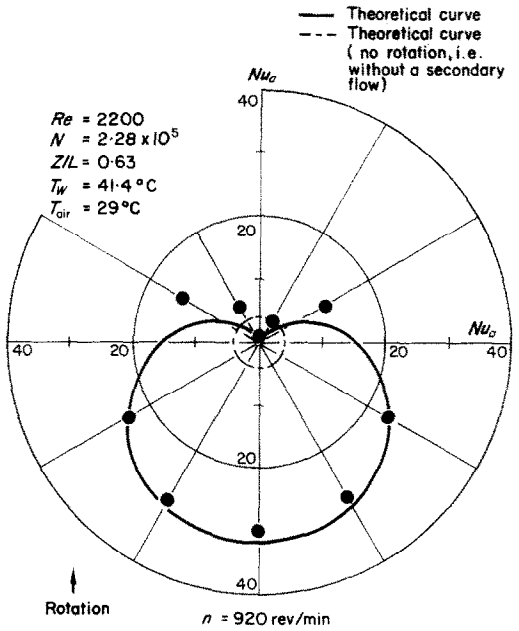

FIG. 10. Local analogous Nusselt number in laminar region (rotation).

and the heat-transfer rate increases in the direction of the action of the Coriolis force.

We vary the speed of rotation and the Reynolds number, which are parameters of these experiments, to make experiments and to plot the results in Fig. 11. The ratio of the mean Nusselt number obtained from further experiments to that for a case without a secondary flow, Nu/Nu_0, is shown on the ordinate in Fig. 11 and the dimensionless parameter describing the influence of the Coriolis force found in the theoretical analysis on the abscissa. The ●-marks represent the results obtained from the mass transfer experiments by using the analogy between heat and mass transfer, the ○-marks the experimental results from heat-transfer experiments, the solid and the dotted lines the theoretical solutions for cases of the constant wall temperature and the constant gradient of wall temperature, respectively. The distribution of the local Nusselt number in the cross section at $Z/L = 0{\cdot}63$ represented by a ⊙-mark corresponds to Fig. 10. These results show that the analogy is established between heat and mass transfer and that the

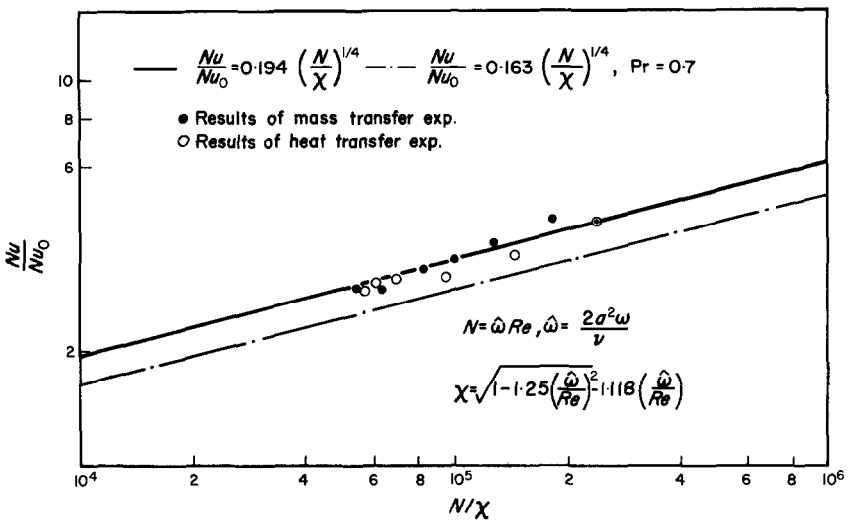

FIG. 11. Heat and mass experimental results in laminar region.

heat-transfer rate in the laminar region increases considerably due to a secondary flow caused by the rotation of the pipe.

5.2. *Experiments in the turbulent region*

(i) *Experiments for calibration (Experiments when a pipe is not rotating).* The distribution of the local analogous Nusselt number in the cross section at $Z/L = 0{\cdot}63$ when a pipe is not rotating is illustrated in Fig. 12 as the calibration in the turbulent region. The solution for a case without a secondary flow is shown by the dotted line. It agrees with the experimental results and they remain the same in the circumferential direction.

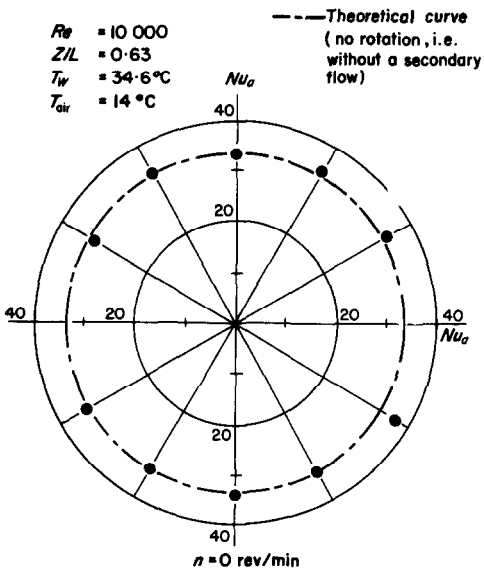

FIG. 12. Local mass transfer result in turbulent region (no rotation).

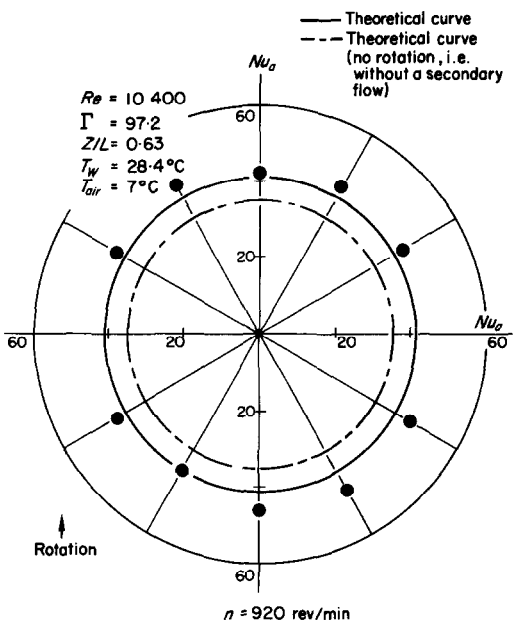

FIG. 13. Local mass transfer result in turbulent region (rotation).

Therefore, the experimental apparatus and the measuring methods are accurate and suitable for the experiments in the turbulent region. (ii) *Experiments when a pipe is rotating.* We give the distribution of the local analogous Nusselt number in the cross section at $Z/L = 0{\cdot}63$ in Fig. 13 as an example of the experimental results when the pipe is rotating. The dotted line denotes the solution for a case without a secondary flow and the solid line the theoretical solution. They agree well with the experimental results. Even though the influence of the secondary flow is seen all over the pipe, an increase in the local Nusselt number at the stagnation point of the secondary flow is not so considerable. It is different from the case in the laminar region in Fig. 10.

We vary the speed of rotation and the Reynolds number to take the ratio of Nu to Nu_0. The results are shown in Fig. 14. We express the

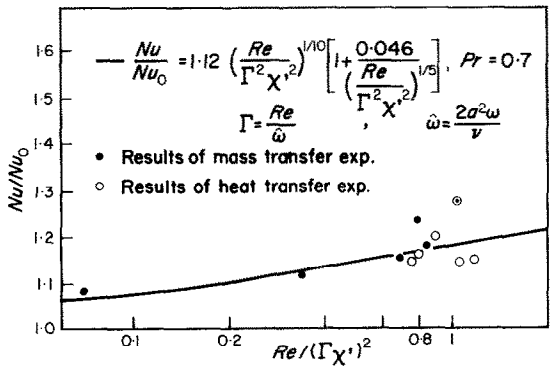

FIG. 14. Heat and mass experimental results in turbulent region.

results of mass transfer the the ●-marks and the experimental solutions of heat transfer by the ○-marks. The solid line describes the theoretical solution reported in this paper, which agrees fairly well with the experimental results. The distribution of the Nusselt number represented by a ⊙-mark in the cross section corresponds to Fig. 13.

The following characteristics are found in the case of the turbulent region from these results: the influence of a secondary flow caused by the Coriolis force is not so considerable in the turbulent region as in the laminar region; though the increase in the mean Nusselt number is more than 10 per cent, the distribution of the local Nusselt number has little variation in the circumferential direction.

6. CONCLUSIONS

In a straight circular pipe rotating around an axis perpendicular to its own axis, the theoretical analysis on the velocity and temperature fields in the fully developed turbulent flow and the experiments on the laminar and turbulent regions were made. We came to the following conclusions from the results. (1) The boundary layer is assumed to appear along the pipe wall in an analysis on the flow in the turbulent region. The resistance coefficient for the fully developed velocity field obtained here is referred to that being in proportion to $Re^{-1/m}$. The value obtained by setting $m = 4$ agrees well with the experimental results. (2) In an analysis on heat transfer in the turbulent region, the Nusselt number is obtained on the assumption that it is in proportion to $Re^{(m-1)/m}\,Pr^{\kappa}$. The ratio of the mean Nusselt number Nu to Nu_0 for a case without a secondary flow is obtained as a function of the dimensionless parameters including the speed of rotation and the Reynolds number. A considerable increase in Nu/Nu_0 is not seen in comparison with the case of the laminar flow, and the local Nusselt number has little variation in the circumferential direction. (3) The experiments on heat and mass transfer were performed by using the naphthalene-sublimation technique. The distributions of the heat-transfer coefficient and the mean heat-transfer coefficient in the circumferential direction in the cross section of the laminar and turbulent regions were obtained. Good agreement was found between the Nusselt number experimentally obtained and the analytical results of the laminar and turbulent regions reported in the first and this paper, respectively.

REFERENCES

1. Y. MORI and W. NAKAYAMA, Convective heat transfer in rotating radial circular pipes (1st report, laminar region). *Int. J. Heat Mass Transfer* **11**, 1027 (1968).
2. H. ITO and K. NANBU, Theoretical study of flow in rotating straight pipes of circular cross section, *Preprint of Annual Meeting of Japan Soc. Mech. Engrs* **194**, 129 (1968).
3. S. N. BARUA, Secondary flow in a rotating straight pipe, *Proc. R. Soc., Lond.* **227A**, 133 (1955).
4. L. TREFETHEN, Flow in rotating radial ducts, G. E. Report No. 55 GL 350-A (1957).
5. H. ITO and K. NANBU, Flow in rotating straight pipes of circular cross section, ASME paper No. 70-WA/FE-13.
6. Y. MORI and W. NAKAYAMA. Study on forced convective heat transfer in curved pipes (2nd report, turbulent region). *Int. J. Heat Mass Transfer* **10**, 37 (1967).
7. Y. MORI and W. NAKAYAMA, Study on forced convective heat transfer in curved pipes (3rd report, Theoretical analysis under the condition of uniform wall temperature and radical formula), *Int. J. Heat Mass Transfer* **10**, 681 (1967).

TRANSFERT PAR CONVECTION THERMIQUE DANS UN TUBE TOURNANT AUTOUR D'UN DIAMETRE D'UNE SECTION DROITE CIRCULAIRE

Résumé—Dans un tube rectiligne à section droite circulaire tournant autour d'un axe perpendiculaire à son propre axe, il apparaît un écoulement secondaire provoqué par la force de Coriolis, ce qui entraine l'augmentation de la résistance à l'écoulement et du flux thermique. On étudie tout d'abord de manière théorique dans cet article la convection thermique turbulente pour des champs de température et de vitesse pleinement développés en supposant une couche limite le long de la paroi. Les accroissements des rapports des nombres de Nusselt Nu/Nu_0 et du rapport des coefficients de frottement λ/λ_0 (les dénominateurs correspondant à l'absence de l'écoulement secondaire) sont moindres pour le cas turbulent que pour le cas laminaire. De plus on montre que le nombre de Nusselt local ne varie pas beaucoup sur la circonférence. On rend compte des résultats expérimentaux concernant le coefficient de transfert thermique et le coefficient de transfert massique local par utilisation de la technique de sublimation du naphtalène pour les régions laminaires et turbulents. Le résultat théorique pour le coefficient de frottement est en accord avec les résultats expérimentaux rapportés ultérieurement. Les résultats expérimentaux présentés sur le transfert thermique sont en bon accord avec la formule théorique relative aux nombres de Nusselt local et moyen donnée dans cet article et dans le premier rapport.

KONVEKTIVE WÄRMEÜBERTRAGUNG IN EINEM RADIAL ROTIERENDEN ZYLINDRISCHEN ROHR.

Zusammenfassung—In einem geraden zylindrischen Rohr, das um eine Achse senkrecht zur Zylinderachse rotiert, entsteht infolge der Corioliskraft eine Sekundärströmung, durch die der Strömungswiderstand und die übertragene Wärmemenge zunimmt. In dieser Arbeit wird erstens unter der Annahme einer Grenzschicht entlang der Rohrwand die turbulente Wärmeübertragung bei voll ausgebildetem Geschwindigkeitsprofil und das Temperaturfeld theoretisch untersucht. Die Zunahme der Verhältnisse der Nusselt-Zahl Nu/Nu_0 und der Reibungskoeffizienten λ/λ_0—wobei sich die Grössen im Nenner auf den Fall ohne Sekundärströmung beziehen—ergab sich dabei kleiner als im laminaren Bereich.

Überdies konnte keine grosse Veränderung der lokalen Nusselt-Zahl über dem Zylinderumfang festgestellt werden.

Als zweites wird über experimentelle Ergebnisse für den Wärmeübergangskoeffizienten und für den lokalen Stoffübergangskoeffizienten, bei Verwendung der Naphthalin-Sublimations-Technik, im laminaren und im turbulenten Bereich berichtet.

Die Übereinstimmung der theoretischen und der experimentellen Werte für den Reibungskoeffizienten wurde schon früher erwähnt. Unsere vorliegenden experimentellen Werte für den Wärmeübergang stimmen überein mit den theoretischen Werten für die lokale und die mittlere Nusselt-Zahl, wie sie in diesem und im ersten Bericht behandelt sind.

КОНВЕКТИВНЫЙ ПЕРЕНОС ТЕПЛА ВО ВРАЩАЮЩЕЙСЯ РАДИАЛЬНОЙ КОЛЬЦЕВОЙ ТРУБЕ

Аннотация—В прямой кольцевой трубе, вращающейся вокруг оси, перпендикулярной своей собственной оси, благодаря кориолисовой силе возникает вторичное течение, из-за которого увеличивается сопротивление потока и скорость переноса тепла. В настоящей работе проведено теоретическое исследование турбулентной тепловой конвекжии при полностью развитых полях скорости и температуры в предположении наличия погранич-

ного слоя вдоль стенки. Найдено, что увеличение отношения числа Нуссельта Nu/Nu_0 и отношения коэффициента трения λ/λ_0 для турбулентного течения, где в знаменатели соотношений входят величины без вторичного потока, меньше, чем в ламинарной области. Кроме того, показано, что не существует больших изменений по окружности локального числа Нуссельта.

Во-вторых, представлены экспериментальные значения коэффициента переноса тепла, а также коэффициента локального переноса массы с помощью сублимации нафталина в ламинарнфх и турбулентных областях. Теоретические значения коэффициента трения согласуются с приведёнными ранее экспериментальными значениями. Экспериментальные данные по переносу тепла, приведенные в данной работе, согласуются с теоретическими формулами для локальных и средних чисел Нуссельта, приведенных в настоящей работе и в первом отчёте.